Int. J. Devl Neuroscience 40 (2015) 1–11

Contents lists available at ScienceDirect

International Journal of Developmental Neuroscience

journal homepage: www.elsevier.com/locate/ijdevneu

Nimodipine enhances neurite outgrowth in dopaminergic brain slice co-cultures

Katja Sygnecka[a,b,*,1], Claudia Heine[a,b,1], Nico Scherf[c], Mario Fasold[d], Hans Binder[d], Christian Scheller[a,e], Heike Franke[b]

[a] Translational Centre for Regenerative Medicine (TRM), University of Leipzig, Philipp-Rosenthal-Straße 55, 04103 Leipzig, Germany
[b] Rudolf Boehm Institute of Pharmacology and Toxicology, University of Leipzig, Härtelstr. 16-18, 04107 Leipzig, Germany
[c] Institute for Medical Informatics and Biometry, Dresden University of Technology, Fetscherstraße 74, 01307 Dresden, Germany
[d] Interdisciplinary Centre for Bioinformatics, University of Leipzig, Härtelstr. 16-18, 04107 Leipzig, Germany
[e] Department of Neurosurgery, University of Halle-Wittenberg, Ernst-Grube-Str. 40, 06120 Halle/Saale, Germany

ARTICLE INFO

Article history:
Received 19 September 2014
Received in revised form 24 October 2014
Accepted 26 October 2014
Available online 4 November 2014

Keywords:
Calcium channel blockade
Development
Neurite growth
Nimodipine
Organotypic slice co-culture
Regeneration

ABSTRACT

Calcium ions (Ca^{2+}) play important roles in neuroplasticity and the regeneration of nerves. Intracellular Ca^{2+} concentrations are regulated by Ca^{2+} channels, among them L-type voltage-gated Ca^{2+} channels, which are inhibited by dihydropyridines like nimodipine. The purpose of this study was to investigate the effect of nimodipine on neurite growth during development and regeneration. As an appropriate model to study neurite growth, we chose organotypic brain slice co-cultures of the mesocortical dopaminergic projection system, consisting of the ventral tegmental area/substantia nigra and the prefrontal cortex from neonatal rat brains. Quantification of the density of the newly built neurites in the border region (region between the two cultivated slices) of the co-cultures revealed a growth promoting effect of nimodipine at concentrations of 0.1 μM and 1 μM that was even more pronounced than the effect of the growth factor NGF.

This beneficial effect was absent when 10 μM nimodipine were applied. Toxicological tests revealed that the application of nimodipine at this higher concentration slightly induced caspase 3 activation in the cortical part of the co-cultures, but did neither affect the amount of lactate dehydrogenase release or propidium iodide uptake nor the ratio of bax/bcl-2. Furthermore, the expression levels of different genes were quantified after nimodipine treatment. The expression of Ca^{2+} binding proteins, immediate early genes, glial fibrillary acidic protein, and myelin components did not change significantly after treatment, indicating that the regulation of their expression is not primarily involved in the observed nimodipine mediated neurite growth. In summary, this study revealed for the first time a neurite growth promoting effect of nimodipine in the mesocortical dopaminergic projection system that is highly dependent on the applied concentrations.

Abbreviations: ANOVA, analysis of variance; Arc, activity-regulated cytoskeleton-associated protein; CBPs, Ca^{2+} binding proteins; DAB, 3,3′-diaminobenzidine hydrochloride; DIV, days *in vitro*; Egr, early growth response protein; FCS, fetal calf serum; Fos, proto-oncogene c-Fos; GFAP, glial fibrillary acidic protein; HS, horse serum; IEGs, immediate early genes; Junb, transcription factor jun-B; LDH, lactate dehydrogenase; LSM, laser scanning microscope; LVCC, L-type voltage-gated Ca^{2+} channels; Mal, myelin and lymphocyte protein; MAP2, microtubule associated protein-2; Mog, myelin oligodendrocyte glycoprotein; MrpL32, mitochondrial ribosomal protein L32; NB-A, Neurobasal-A; NGF, nerve growth factor; P, postnatal day; PFC, prefrontal cortex; PI, propidium iodide; Plp1, myelin proteolipid protein 1; Pvalb, parvalbumin; qPCR, quantitative reverse transcription polymerase chain reaction; SOM, self-organizing maps; TBS, tris buffered saline; Ubc, ubiquitin; VTA/SN, ventral tegmental area/substantia nigra.

* Corresponding author at: Rudolf Boehm Institute of Pharmacology and Toxicology, University of Leipzig, Härtelstr. 16-18, 04107 Leipzig, Germany. Tel.: +49 0341 97 24606; fax: +49 0341 97 24609.
E-mail addresses: katja.sygnecka@trm.uni-leipzig.de (K. Sygnecka), claudia.heine@trm.uni-leipzig.de (C. Heine), nico.scherf@tu-dresden.de (N. Scherf), mario@bioinf.uni-leipzig.de (M. Fasold), binder@izbi.uni-leipzig.de (H. Binder), christian.scheller@medizin.uni-halle.de (C. Scheller), heike.franke@medizin.uni-leipzig.de (H. Franke).
[1] Both authors contributed equally to the study.

http://dx.doi.org/10.1016/j.ijdevneu.2014.10.005
0736-5748/

1. Introduction

Nimodipine is a blocker of the L-type voltage-gated Ca^{2+} channels (LVCC), which regulate the intracellular Ca^{2+} concentration. Calcium ions (Ca^{2+}) play an important role in neuronal plasticity (Gispen et al., 1988). Their intracellular concentration is crucial for the regulation of axonal and dendritic growth, guidance during neuronal development and for resprouting of axons after injury (for review see Gomez and Zheng, 2006). It has been shown that proper neuronal development proceeds when the intracellular Ca^{2+} is within an optimal range (Fields et al., 1993; Kater and Mills, 1991; Kater et al., 1988). Therefore, the modulation of Ca^{2+} channels such as the LVCC is of special interest, when neurite (re)growth is desired.

Being one of the examined LVCC blockers, the dihydropyridine derivate nimodipine has been intensively studied. Its beneficial effects have been confirmed in clinical studies (Liu et al., 2011, Scheller and Scheller, 2012) and in diverse experimental studies, where it has been applied to models of various disorders. These experimental studies, analyzing the effect of nimodipine (and other dihydropyridine LVCC blockers), focused on (i) the neuroprotective properties after different kinds of neuronal injury (Harkany et al., 2000; Krieglstein et al., 1996; Lecht et al., 2012; Li et al., 2009; Rami and Krieglstein, 1994; Weiss et al., 1994), for example by reducing the consequent intracellular free Ca^{2+} overload after *e.g.* ischemic injury and excitotoxic lesion (Kobayashi and Mori, 1998) and (ii) the neurite growth promoting characteristics, mainly investigated in the peripheral nervous system (Angelov et al., 1996; Lindsay et al., 2010; Mattsson et al., 2001).

LVCC are expressed in a couple of brain regions of the central nervous system, among them the mesencephalon (Mercuri et al., 1994; Nedergaard et al., 1993; Takada et al., 2001), the cortex, and the hippocampus (Dolmetsch et al., 2001; Quirion et al., 1985; Tang et al., 2003). In the cortex, LVCC are located on the entire postnatal neuron including dendrites and axonal processes (Tang et al., 2003).

Although the beneficial outcomes of LVCC modulation by nimodipine are well established, the exact cellular and molecular mechanisms by which this modulation occurs are still unclear. Nevertheless, results of some previously published studies may in part explain how neurite growth after nimodipine treatment is accomplished. An upregulation of Ca^{2+} binding proteins (CBPs, parvalbumin (Pvalb), S100b, calbindin) has been observed in cortical neurons after nimodipine administration (Buwalda et al., 1994; Luiten et al., 1994). Furthermore, the expression of the glial fibrillary acidic protein (GFAP) was enhanced following long-term nimodipine treatment (Guntinas-Lichius et al., 1997). An increase in myelination was found surrounding the recovering neurons after unilateral facial crush injury and interestingly also around neurons located in the contralateral nonlesioned site in nimodipine treated animals (Mattsson et al., 2001). Moreover, microglial-mediated oxidative stress and inflammatory response was attenuated by nimodipine (but not by other LVCC blockers) in dopaminergic neurons/microglial co-cultures (Li et al., 2009).

In this study, we wanted to investigate whether nimodipine directly influences neurite growth. We further aimed to elucidate which genes are potentially involved in the nimodipine mediated growth effects. To address these questions, we determined the neurite density in the border region of organotypic co-cultures of the mesocortical dopaminergic system, which culture together brain slices of the ventral tegmental area/substantia nigra (VTA/SN) and prefrontal cortex (PFC) (Heine et al., 2007; Heine and Franke, 2014), and analyzed gene expression patterns of nimodipine treated samples and control samples.

Our findings indicate that nimodipine, at appropriate dosages, is a promising substance to enhance neurite outgrowth as shown in the applied co-culture model of the dopaminergic (CNS)-projection system.

2. Experimental procedures

2.1. Materials

The solvent ethanol was purchased from AppliChem GmbH (Darmstadt, Germany) and VWR International (Dresden, Germany), respectively. Glutamate, nerve growth factor (NGF), and staurosporine were purchased from Sigma–Aldrich Co. (St. Louis, MO, USA). Nimodipine (pure substance) was a gift from Bayer Vital GmbH (Leverkusen, Germany). 1000-fold stock solutions of nimodipine were prepared in absolute ethanol and finally added to 1 ml of incubation medium (resulting ethanol concentration 0.1%, details see Section 2.3). Untreated cultures ("untreated") or cultures treated with the vehicle ethanol ("ethanol", resulting end concentration 0.1%) were used as control groups.

2.2. Animals

Neonatal rat pups (WISTAR RjHan, own breed; animal house of the Rudolf Boehm Institute of Pharmacology and Toxicology, University of Leipzig) of postnatal day 1–4 (P1-4) were used for the preparation of the organotypic slice co-cultures. The animals were housed under standard laboratory conditions of 12 h light–12 h dark cycle and allowed free access to lab food and water *ad libitum*.

All of the animal use procedures were approved by the Committee of Animal Care and Use of the relevant local governmental body in accordance with the law of experimental animal protection. All efforts were made to minimize animal suffering and to reduce the number of animals used.

2.3. Preparation, culture and treatment of slice co-cultures

Dopaminergic brain slice co-cultures were prepared from P1-4 rats and cultured according to the "static" culture protocol described previously (Heine et al., 2007; Heine and Franke, 2014). In brief, coronal sections (300 μm) were cut at mesencephalic and forebrain levels using a vibratome (Leica, Typ VT 1200S, Nussloch, Germany). For details see also supplementary Fig. S1. After separation of VTA/SN and PFC, respectively, the slices were transferred into petri dishes, filled with cold (4 °C) preparation solution (Minimum Essential Medium (MEM) supplemented with glutamine (final concentration 2 mM) and the antibiotic gentamicin (50 μg/ml); all from Invitrogen GmbH, Darmstadt, Germany). Thereafter, the selected sections were placed as co-cultures (VTA/SN + PFC, 4 co-cultures per well) on moistened membrane inserts (0.4 μm, Millicell-CM, Millipore, Bedford, MA, USA) in 6-well plates (Fig. S1.A3), each filled with 1 ml incubation medium (50% Minimal Essential Medium, 25% Hank's Balanced Salt Solution, 25% heat inactivated horse serum (HS), 2 mM glutamine and 50 μg/ml gentamicin; all from Invitrogen GmbH supplemented with 0.044% sodium bicarbonate, Sigma-Aldrich; pH was adjusted to 7.2), referred to as "25% HS incubation medium".

Supplementary Fig. S1 can be found, in the online version, at http://dx.doi.org/10.1016/j.ijdevneu.2014.10.005.

The preliminary gene expression studies (microarray analysis, quantitative reverse transcription polymerase chain reaction, qPCR) have been conducted after culture under serum-free culture conditions. Therefore, after 4 days *in vitro* (DIV) the 25% HS incubation medium was replaced by serum-free medium (Neurobasal-A (NB-A) medium, 1 mM glutamine supplemented with 2% B27 and 50 μg/ml gentamicin; all from Invitrogen GmbH), referred to as "NB-A incubation medium". Nimodipine (final concentration 10 μM) or the vehicle ethanol (0.1%), respectively were added to the incubation medium at DIV4, 6, 8 and 11.

To determine the concentration of nimodipine that would be appropriate, we first analyzed previous published studies and the therein used concentrations (10 μM: Blanc et al., 1998; Krieglstein et al., 1996; Lecht et al., 2012; Tang et al., 2003; 20 μM: Martínez-Sánchez et al., 2004; Pisani et al., 1998; Pozzo-Miller et al., 1999; 50 μM: Bartrup and Stone, 1990, toxic at higher concentrations: Turner et al., 2007). Second, we quantified nimodipine uptake into the co-cultures with applied nimodipine concentrations ranging from 10 μM to 40 μM in a preliminary experiment. We found the lowest dose applied (10 μM nimodipine in the culture medium) yielded a sufficiently high concentration in the tissue (unpublished results). Therefore, the following studies were at first conducted with 10 μM nimodipine.

The analysis of neurite growth in the organotypic brain slice co-cultures is a well-established technique in our lab (Heine et al., 2013; Heine et al., 2007). Therefore, the neurite growth analysis has been performed after culture in 25% HS incubation medium. For the neurite growth quantification, slice co-cultures were divided into different experimental groups and were treated with nimodipine at different concentrations (first 10 μM, later 0.1 μM and 1 μM) or the vehicle control ethanol. A second control group was left untreated. Nimodipine and ethanol were added directly after the preparation and at each medium change at DIV1,4,6 and 8 (Fig. 1). In a second study the effect of 1 μM nimodipine alone or in combination with 50 ng/ml NGF (final concentration) was compared to 50 ng/ml NGF alone. These culture conditions (25% HS incubation medium, substance application five times as indicated in Fig. 1) were also applied for toxicity tests and later gene expression studies. In addition, tissue slices of the nimodipine treated groups were dissected

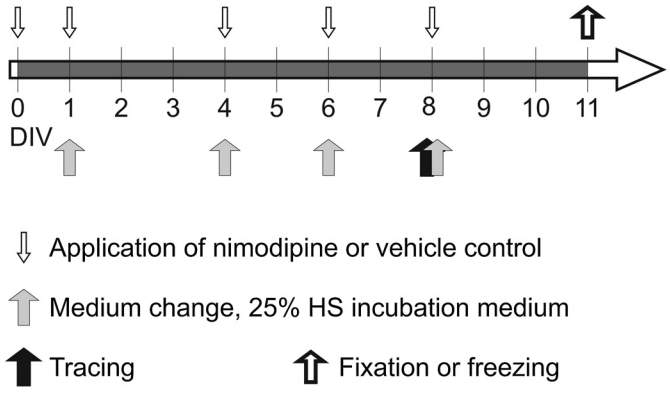

Fig. 1. Culture and treatment schedule. For neurite growth, toxicity and later gene expression analysis, nimodipine or ethanol were applied at day *in vitro* (DIV)0, 1, 4, 6 and 8. Neurite growth was quantified after biocytin tracing at DIV8 and fixation at DIV11, as indicated. For the analysis of toxicity and gene expression, co-cultures were harvested at DIV11.

in nimodipine containing preparation medium. This is in accordance to *in vivo* data of a human study, where prophylactic treatment had the strongest beneficial effect (Scheller et al., 2012). For this reason, 36 nM nimodipine were added to the preparation solution on the basis of findings in the literature (Lindsay et al., 2010).

2.4. Analysis of gene expression

2.4.1. RNA extraction and quality control

RNA extraction was performed for microarray analysis and quantitative reverse transcription polymerase chain reaction (qPCR). At the end of culture, both regions of the co-cultures (PFC and VTA/SN) were separated with a scalpel and all PFC- and VTA/SN-slices from one well, containing four co-cultures, were pooled to one sample, respectively. Afterwards total RNA was isolated using TRIzol reagent (Life Technologies, Gaithersburg, MD, USA) according to the manufacturer's instructions. The total RNA was alcohol precipitated for a second time with addition of ammonium acetate and GlycoBlue (Life Technologies) for optimal recovery of the nucleic acids. RNA integrity and concentration for each sample that was later on applied to the microarray, was examined on an Agilent 2100 Bioanalyser (Agilent Technologies, Palo Alto, CA, USA) using the RNA 6.000 LabChip Kit (Agilent Technologies) according to the manufacturer's instructions. RNA integrity and concentration of samples, that were investigated by qPCR, were examined on a 1.5% agarose gel and with NanoDrop1000 (NanoDrop Technologies, Wilmington, DE, USA), respectively.

2.4.2. Microarray analysis

Microarray measurements were conducted at the microarray core facility of the Interdisziplinäres Zentrum für klinische Forschung (IZKF) Leipzig (Faculty of Medicine, University of Leipzig). Biotin labeled probes were prepared from 250 ng of total RNA using the TargetAmp™-Nano Labeling Kit for Illumina® Expression BeadChip (Biozym, Hessisch Oldendorf, Germany) according to the manufacturer's instructions. Hybridization of labeled probes to an Illumina Rat Ref12 BeadChip (Illumina Inc., San Diego, CA, USA) using the respective BeadChip kit (Illumina) was done according to the protocol of the manufacturer. Bead level data was preprocessed using standard Illumina software resulting in background-corrected, quantile-normalized expression estimates which were used for further analysis. Ranked lists of differentially expressed genes were obtained in treatment-*vs.*-control comparisons and judged using the Welch's *t*-test and subsequent *False Discovery Rate adjustment* (Opgen-Rhein and Strimmer, 2007). *Gene Set Z-scoring* (Törönen et al., 2009) was used to perform gene set analysis using gene-ontology terms (Wirth et al., 2012).

2.4.3. qPCR

Reverse transcription was performed using the RevertAid™ H Minus First Strand cDNA Synthesis Kit (Fermentas, St. Leon-Rot, Germany) with 1 μg total RNA and oligo(dT)$_{18}$ primer. qPCR was conducted using a LightCycler (Roche Diagnostics, Mannheim, Germany) in a total volume of 10 μl per capillary containing 5 μl QuantiTect SYBR Green 2× Master Mix (Roche), 0.4 μl cDNA, 1 μl primer (5 μM, each) specific for the different target genes or the reference genes (mitochondrial ribosomal protein L32, MrpL32 and ubiquitin, Ubc) and 3.6 μl water. The oligonucleotide primer sequences are listed in Table A.1. The Hot Start Polymerase was activated by a 15 min pre-incubation at 95 °C, followed by 55 amplification cycles at 95 °C for 10 s, 60 °C for 10 s and 72 °C for 10 s. The obtained crossing point (CP) values were between 15 and 28 for the different target genes. A melting curve analysis was performed to verify correct qPCR products. The following appropriate controls have been used: no template control (water) and "reverse transcription-minus control", in order to exclude the presence of genomic DNA in the samples. Quantification of gene expression was performed by the ΔCP method with MrpL32 and Ubc serving as reference housekeeping genes.

2.5. Neurite quantification

2.5.1. Tracing and neurite visualization

To quantify neurite outgrowth between the two slices of the co-cultures, biocytin-tracing (detailed time schedule in Fig. 1) was performed according to a previously described protocol (Franke et al., 2003; Heine et al., 2007). At DIV8, small biocytin-crystals of similar size were placed onto the VTA/SN slice of the co-cultures. Co-cultures were left in contact with the crystals for 2 h to allow the uptake of biocytin. Afterwards they were reincubated with medium containing the respective nimodipine concentrations for 48 h. At DIV11, the cultures were fixed and cut into 50 μm vibrosections. Afterwards, the anterograde tracer biocytin was labeled using the avidin–biotin-complex (1:50, ABC-Elite Kit, Vector Laboratories, Inc., Burlingame, CA, USA), in combination with nickel/cobalt-intensified 3.3′-diaminobenzidine hydrochloride (DAB; Sigma–Aldrich) as a chromogen. After mounting on glass slides, all stained sections were dehydrated in a series of graded ethanol, processed through n-butylacetate and covered with Entellan (Merck, Darmstadt, Germany).

2.5.2. Automated image quantification

The quantification of outgrowing biocytin-traced neurites was performed as previously described (Heine et al., 2013; Heine and Franke, 2014). Briefly, microscopic images were taken at 40-fold magnification in the border region (where the two initially separated brain slices were grown together, for details see also Fig. S1.B1) using an usual transmitted light bright field microscope (Axioskop 50; Zeiss Oberkochen, Germany) equipped with a CCD camera (DCX-950P, SONY Corporation, Tokyo, Japan). The following criteria were used for the selection of the biocytin-traced slices: (a) the tracer was correctly placed on the VTA/SN, (b) the major part of the VTA/SN was characterized by a dense network of biocytin-traced structures and (c) no traced cell bodies had been observed in the target region PFC (in more detail described in Heine et al., 2007). During image acquisition, preceding treatments of the observed tissue slices were hidden from the experimenter.

After pre-processing of the images (for details see Heine et al., 2013), neurite structures appeared as well-defined bright regions. Subsequently, the image area occupied by the neurites was measured to obtain a reasonable estimate of the underlying neurite density of the analyzed specimens. Precisely, the ratio of the number of foreground pixels (neurites) against the total number of pixels in the images was taken, giving the percentage of area occupied by neurites in the focal plane. Neurite density was subsequently normalized to the median values of the untreated controls of each individual experiment.

2.6. Analysis of cell death

2.6.1. Lactate dehydrogenase (LDH) activity in conditioned culture medium

LDH release into the 25% HS incubation medium was quantified after treatment with 0.1 μM, 1 μM and 10 μM (time schedule according to Fig. 1). Medium samples were collected at every medium exchange (DIV1, 4, 6, 8) and before fixation (DIV11), and stored at −20 °C until further analysis.

When the samples reached room temperature after thawing, LDH activity was measured by the method of Koh and Choi (1987) applied to 96-well plate format using filter-based plate reader device (Polarstar Omega von BMG Labtech, Offenburg, Germany) measuring the absorption at 340 nm. Briefly, the LDH substrate pyruvate and the coenzyme NADH (both Sigma–Aldrich) were added to the conditioned medium samples and the decrease of NADH due to LDH activity was measured over the time (every 10 s for 3 min).

To exclude variations due to temperature changes between individual sets of measurements, LDH activity of all samples has been normalized to the control sample (untreated) at DIV1 of the respective preparation.

2.6.2. Active caspase 3 immunolabeling and propidium iodide (PI) uptake

For the active caspase 3 immunolabeling and PI (Invitrogen GmbH) uptake quantification, nimodipine was applied at 0.1 μM, 1 μM and 10 μM as described above for the neurite quantification study. As positive controls for caspase 3 activation and the induction of necrosis, 5 μM staurosporine (for 4 h) and 10 mM glutamate (for 48 h), respectively, have been added to the incubation medium prior to fixation of the co-cultures at DIV11. PI (7.5 μM) was added 3 h before the fixation to every culture well.

After fixation, co-cultures were cut into 50 μm slices as described above and stained. In detail, slices were blocked with Tris buffered saline (TBS, 0.05 M; pH 7.6) containing fetal calf serum (FCS, 5%) and Triton X-100 (0.3%) for 30 min. Then, the slices were incubated with a primary antibody directed against active caspase 3 (produced in rabbit, 1:50, MBL International, Inc., Woburn, MA, USA) for 48 h at 4 °C. After washing with TBS, the secondary antibody (donkey anti rabbit Alexa488 conjugated IgG, 1:400, Jackson ImmunoResearch, West Grove, PA, USA), diluted in TBS supplemented with 5% FCS and 0.3% Triton X-100, was applied for 2 h at room temperature. For further characterization of active caspase 3 positive cells, multiple fluorescence labeling was performed. The slices were incubated with a mixture of primary antibodies (rabbit anti-active caspase 3, 1:50, MBL International,

in combination with mouse anti-microtubule associated protein-2 (MAP2), 1:1000, Millipore, Temecula, CA, USA and goat anti-GFAP, 1:1000, Santa Cruz Biotechnology, Inc., Santa Cruz, CA, USA) for 48 h at 4 °C. After washing with TBS, the secondary antibodies (donkey anti rabbit Cy3 conjugated IgG, 1:1000 and donkey anti mouse Alexa488 conjugated IgG, 1:400 and donkey anti goat Dyelight 647 conjugated IgG, all Jackson ImmunoResearch, West Grove, PA, USA), diluted in TBS supplemented with 5% FCS and 0.3% Triton X-100, was applied for 2 h at room temperature. In addition, slices were stained with the nucleic acid probe Hoechst 33342 (40 μg/ml, Molecular Probes, Leiden, Netherlands), to identify the cell nuclei. After mounting on glass slides, all stained sections were dehydrated and covered as described above.

2.6.3. Image analysis

Fluorescence labeled specimens were imaged with a confocal laser scanning microscope (LSM 510 Meta; Zeiss, Oberkochen, Germany). Excitation wavelengths were 633 nm, 543 nm, 488 nm and 351 nm/364 nm to evoke the Dyelight 647, PI, Alexa488 and Hoechst fluorescence, respectively. Microscopic images were taken at 20-fold magnification. For each group, 6 slices were analyzed within the PFC and VTA/SN, (3 pictures per slice and region, resulting in 18 pictures per group and region). During image acquisition and manual cell counting preceding treatments of the observed tissue slices were hidden from the experimenter. Cells positive for active caspase 3 were counted manually with the help of ImageJ *cell counter* plugin (http://rsb.info.nih.gov/ij/; http://rsbweb.nih.gov/ij/plugins/cell-counter.html). PI uptake quantification was conducted with an algorithm implemented in Wolfram Mathematica 9.0.1. To assess the number of PI positive cell nuclei, a global threshold for binarization was chosen to divide the image in PI positive nuclei and background. Furthermore, a maximal particle size was defined to estimate the number of cell nuclei in regions where the segmentation could not separate single nuclei. In those cases, the area of the region was divided by the mean cell size (which was determined from a visually verified image), to obtain a rough estimate of the number of cells which are connected in this region.

2.7. Statistics

All quantitative data (except microarray analysis) has been analyzed with SigmaPlot 12 statistical analysis program. Details referring to the applied tests are specified in the respective result section and in the figure legends.

3. Results

3.1. Upregulation of immediate early genes (IEGs) in the PFC after treatment with 10 μM nimodipine

To elucidate the mode of action of nimodipine, we conducted a microarray study to preliminarily identify the genes whose expression is modulated by nimodipine application. After substance application (4 times 10 μM, for details regarding the chosen concentration see Section 2.3), co-cultures were separated into PFC and VTA/SN. The two regions were analyzed individually. Gene expression patterns of untreated, vehicle control ethanol, or nimodipine treated samples were compared. There were no differentially expressed genes in the VTA/SN, but we found upregulated genes in the nimodipine treated PFC samples. Therefore, we focused on the PFC samples for further gene expression analyses.

Self-organizing map (SOM) analysis of the microarray data was used to visualize the expression patterns of each sample that has been applied to the microarray. The comparison of the SOMs revealed that the expression patterns of both controls (untreated and ethanol) were very similar to each other. Therefore, the samples of the two groups were combined to a single control group for further analysis of the microarray study. Differential expression analysis of nimodipine *versus* control group within the PFC yielded seven genes with log fold changes > 2 ($\log_2$ FC, p-value Welch's t-test): Arc (activity-regulated cytoskeleton-associated protein, $\log_2$ FC 3.487, $p = 0.018$), Egr1 (early growth response protein 1, $\log_2$ FC 2.466, $p = 0.06$), Egr2 ($\log_2$ FC 3.568, $p = 0.095$), Egr4 ($\log_2$ FC 2.844, $p = 0.177$), Fos (proto-oncogene c-Fos, $\log_2$ FC 2.05, $p = 0.219$), JunB (transcription factor jun-B, $\log_2$ FC 2.069, $p = 0.280$), and Pmch (pro-MCH precursor, $\log_2$ FC 2.853, $p = 0.499$). The transcripts of the IEGs (Arc, Egr1,2,4, Fos and JunB) were quantified by qPCR of five independent preparations. With the exception of JunB, significantly higher gene expressions were confirmed after nimodipine treatment, with median values ranging from 5-fold to 36-fold compared to vehicle control ethanol, Mann–Whitney rank sum test, $p < 0.05$, $p < 0.01$ (Fig. 2). All of these validated upregulated genes belong to the group of IEGs. The transcriptional activation of these genes after nimodipine treatment, which are involved in neurite growth and plasticity (reviewed in Pérez-Cadahía et al., 2011; Shepherd and Bear, 2011) strongly suggested a nimodipine induced enhancement in neurite growth in our test system under the applied conditions.

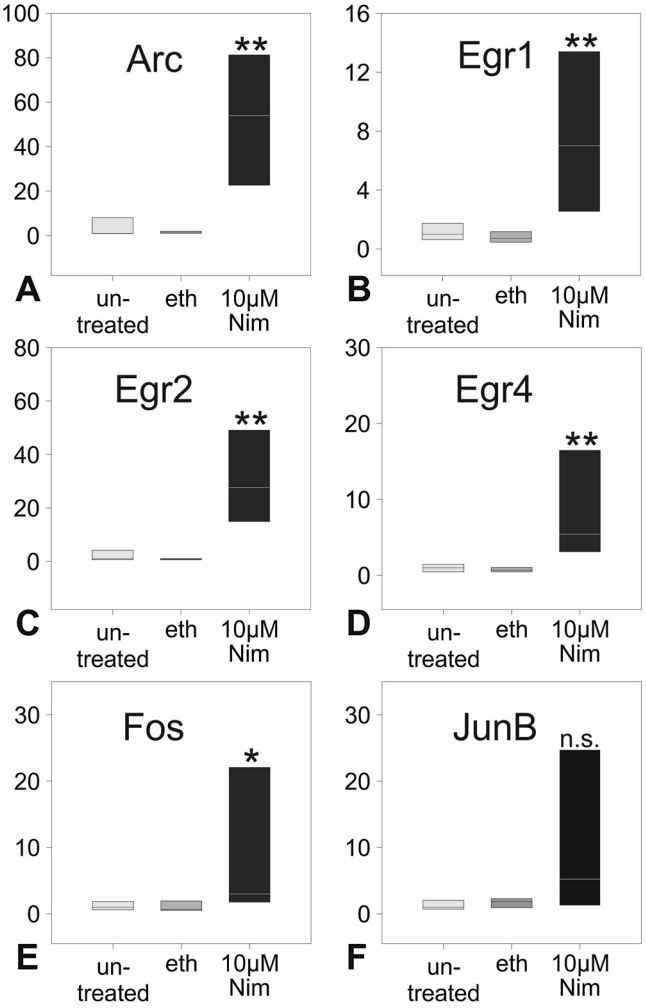

Fig. 2. Results of qPCR validation experiments. (A–F) Expression levels of the IEGs, which were found to be upregulated in the PFC in the microarray study: Arc, activity-regulated cytoskeleton-associated protein; Egr1,2 and 4, early growth response protein 1, 2 and 4; Fos, proto-oncogene c-Fos; Junb, transcription factor jun-B are expressed as ΔCP, normalized to untreated control (y-axis), while x-axis represents the different treatments (application of 0.1% ethanol (in the figure: eth) or 10 μM nimodipine (in the figure: Nim), respectively at DIV4, 6, 8 and 11). Statistical analysis was done in comparison to vehicle control ethanol. (A–E) Treatment with 10 μM nimodipine increased expression of the investigated genes of interest significantly. Data are shown as box plots, n(independent samples) = 5, $^*p < 0.05$, $^{**}p < 0.01$, Mann–Whitney rank sum test.

3.2. No enhanced neurite growth after treatment with 10 μM nimodipine

In parallel to preliminary gene expression analysis, we investigated whether nimodipine may enhance neurite growth in the dopaminergic system. Therefore a treatment study with 10 μM nimodipine in comparison to untreated and vehicle ethanol treated control co-cultures was performed, following a well-established treatment schedule for neurite growth analysis (Fig. 1 and Heine et al., 2007, 2013). Surprisingly, treatment with nimodipine at this concentration did not enhance neurite growth in the border region

(for details see Fig. S1) of the co-cultures. Automated image quantification of at least 60 analyzed pictures per group revealed that the median value for neurite density in 10 μM nimodipine treated co-cultures was even lower than neurite density in the vehicle control (10 μM nimodipine was 85% of ethanol group, $p = 0.283$; Mann–Whitney rank sum test, data not shown).

3.3. 10 μM nimodipine induces an increase in active caspase 3 positive cells, but has no influence on PI uptake, LDH release and bax/bcl-2 ratio

We wanted to clarify whether the application of 10 μM nimodipine to the co-cultures induces (neuro-)toxic effects. Different toxicological methods have been used after application of 0.1 μM, 1 μM, and 10 μM nimodipine (according to the treatment schedule shown in Fig. 1) to quantify apoptotic and necrotic cell death: (i) measurement of LDH release into the incubation medium, (ii) PI uptake quantification, (iii) analysis of caspase 3 activation in immunostained co-culture slices, and (iv) calculation of the bax/bcl-2 ratio.

The highest LDH activity was detected at DIV1 (Fig. 3A). It decreased during the culture period without a significant difference between the differently treated groups. These findings are substantiated by the analysis of PI uptake into the PFC and the VTA/SN, where no significant changes were observed after the different treatments, except in the positive control treated with glutamate (10 mM, 48 h). Data are shown in Fig. 3B.

Moreover, the number of the active caspase 3 positive cells was quantified after immunofluorescence labeling (exemplary microscopic images are shown in Fig. 3D–F). We found a slightly but significantly increased number of cells being positive for active caspase 3 staining after treatment with nimodipine (10 μM) in the cortical part of the cell culture compared to the vehicle ethanol treated control ($p < 0.05$). In comparison, the positive control staurosporine, which is known to induce apoptosis, was characterized by an obviously much higher number of active caspase 3 positive cells ($p < 0.01$); n(analyzed images) = 18, ANOVA on ranks followed by all pairwise multiple comparison procedures (Dunn's test) (Fig. 3C). To assess apoptosis with a second method, expression levels of bax and bcl-2 were quantified and bax/bcl-2 ratio was calculated for all different treatments (untreated, ethanol, nimodipine (0.1–10 μM)) in PFC and VTA/SN samples. In contrast to active caspase 3 immunoreactivity, no significant changes were detected between the different groups (data not shown).

With multiple fluorescence labeling, we further aimed to characterize the identity of the cells being apoptotic after application of 10 μM nimodipine. Active caspase 3 positive cells are often surrounded by GFAP positive structures (Fig. 3G). Additionally, we found active caspase 3 immunoreactivity and apoptotic fragmentation of cell nuclei (Fig. 3G, insert) located in areas where MAP2 staining is less defined (Fig. 3H,I), indicating a locally restricted loss of MAP2 immunoreactivity during apoptosis.

3.4. Significant enhancement of neurite growth after treatment with 0.1 μM and 1 μM nimodipine

After having shown that 10 μM nimodipine induces caspase 3 activation in the organotypic brain slice co-cultures whereas 0.1 μM and 1 μM do not, the neurite growth promoting potential of nimodipine was investigated again by applying these lower concentrations to the co-cultures (according to the time schedule of treatment in Fig. 1). After application of nimodipine at both concentrations (0.1 μM, 1 μM), a visible increase in biocytin-traced outgrowing neurites in the border region of the co-cultures was observed in comparison to control conditions (untreated control, ethanol; Fig. 4A). In contrast, neurite density after the application of 10 μM nimodipine is as low as in the images of the controls (Fig. 4A). These qualitative observations have been confirmed by automated image quantification, revealing a significant augmentation of the neurite density in co-cultures which had been treated with 0.1 μM and 1 μM nimodipine (116% and 127% of vehicle control ethanol, respectively), n(analyzed images) > 225, $p < 0.01$, ANOVA on ranks followed by all pairwise multiple comparison procedures (Dunn's test) (Fig. 4B).

For a better estimation of the neurite growth promoting impact of nimodipine in our co-culture system, the effect of 1 μM nimodipine was compared to the well-known growth factor NGF. To check additionally for potential synergistic action, both compounds were also applied together. The strongest effect was observed for the combination of both compounds (138% of vehicle control ethanol), followed by 1 μM nimodipine (127% of vehicle control ethanol) and NGF alone (119% of vehicle control ethanol), (see supplementary Fig. S2). All of these treatments were significantly higher than the vehicle control ethanol ($p < 0.01$). The combination of nimodipine (1 μM) and NGF was significantly higher than NGF alone ($p < 0.05$) but not significantly higher than 1 μM nimodipine, n(analyzed images) > 173, ANOVA on ranks followed by all pairwise multiple comparison procedures (Dunn's test).

Supplementary Fig. 2 can be found, in the online version, at http://dx.doi.org/10.1016/j.ijdevneu.2014.10.005.

3.5. Expression levels of CBPs, IEGs and myelin constituents are not altered by 0.1 μM and 1 μM nimodipine

With neurite density quantification, we did show a neurite growth promoting effect of nimodipine (0.1 μM, 1 μM) in the dopaminergic projection system. Nevertheless, the mode of action remained unclear and we wanted to address this issue. After culture under the conditions, where enhanced neurite outgrowth was found, we quantified the changes in expression levels of several genes in PFC and VTA/SN separately (Fig. 5 exemplarily shows the results for the PFC, treatment according to Fig. 1): (i) The CBPs Pvalb and S100b have been reported to be upregulated after nimodipine treatment (Buwalda et al., 1994; Luiten et al., 1994). Our results revealed no significant changes in gene expression in our model in response to nimodipine application. (ii) It was shown that nimodipine treatment causes an increase in the thickness of the myelin sheath (Mattsson et al., 2001). Therefore, we quantified expression levels of the myelin constituents myelin and lymphocyte protein (Mal), myelin oligodendrocyte glycoprotein (Mog) and myelin proteolipid protein 1 (Plp1). Again, no significant changes in gene expression were found. (iii) Guntinas-Lichius et al. (1997) described a nimodipine induced increase in transcripts of GFAP. We quantified GFAP in our experimental model, detecting no significant change in expression levels. (iv) Furthermore, we tested if the IEGs that were found to be up-regulated in the microarray will also be up-regulated under the conditions that lead to enhanced neurite growth. The findings from the microarray and subsequent qPCR validation (with 10 μM nimodipine) were not confirmed after culture under neurite growth conditions. We found that the expression of Arc, Egr1, Egr2, Fos and Junb was not significantly changed after treatment with nimodipine (0.1 μM, 1 μM). Nevertheless, there is a tendency of a concentration dependent reduction of expression levels of the above mentioned genes, which was significant for Egr4 after application of 1 μM nimodipine, n(independent samples) = 6 for all analyzed transcripts (Fig. 5).

4. Discussion

We investigated the effects of nimodipine in an organotypic co-culture model of the dopaminergic system and we found

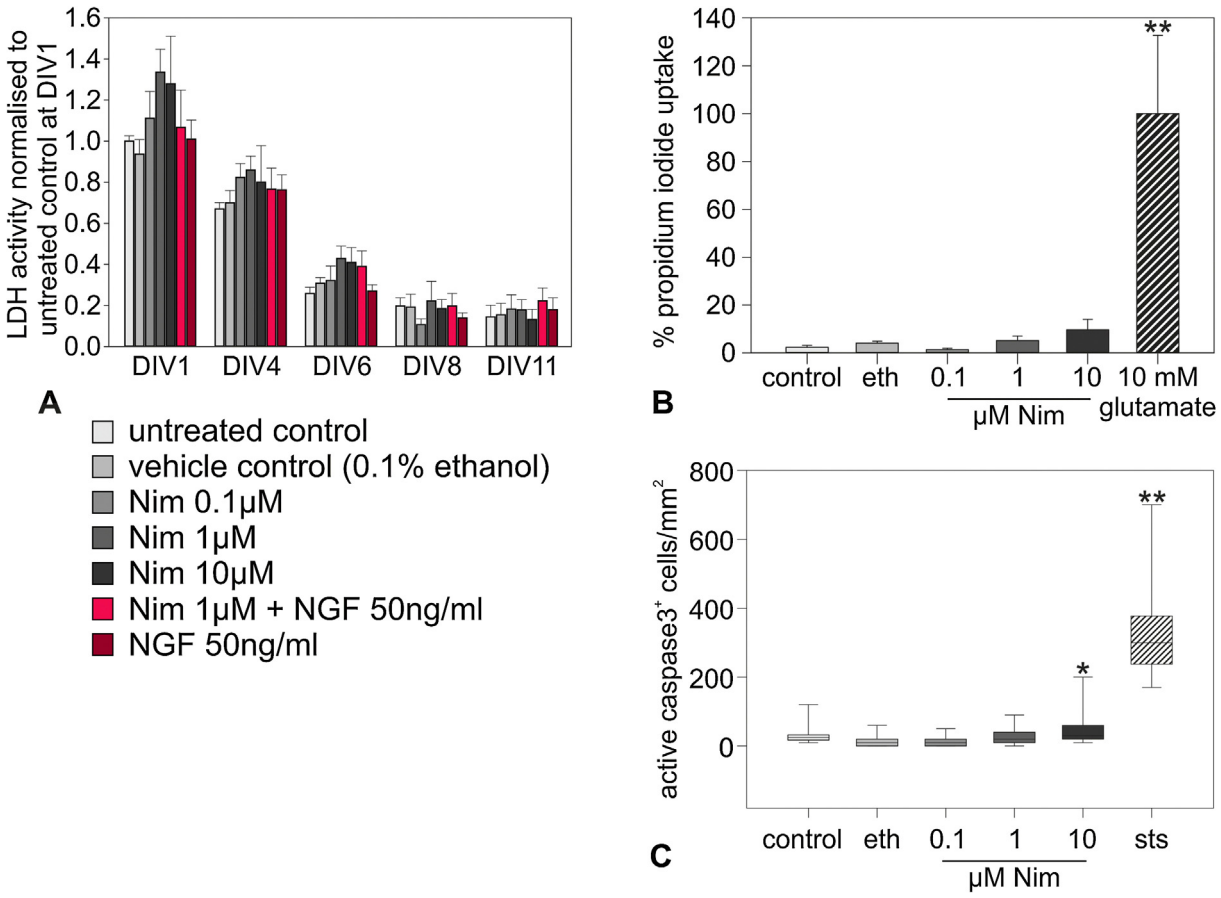

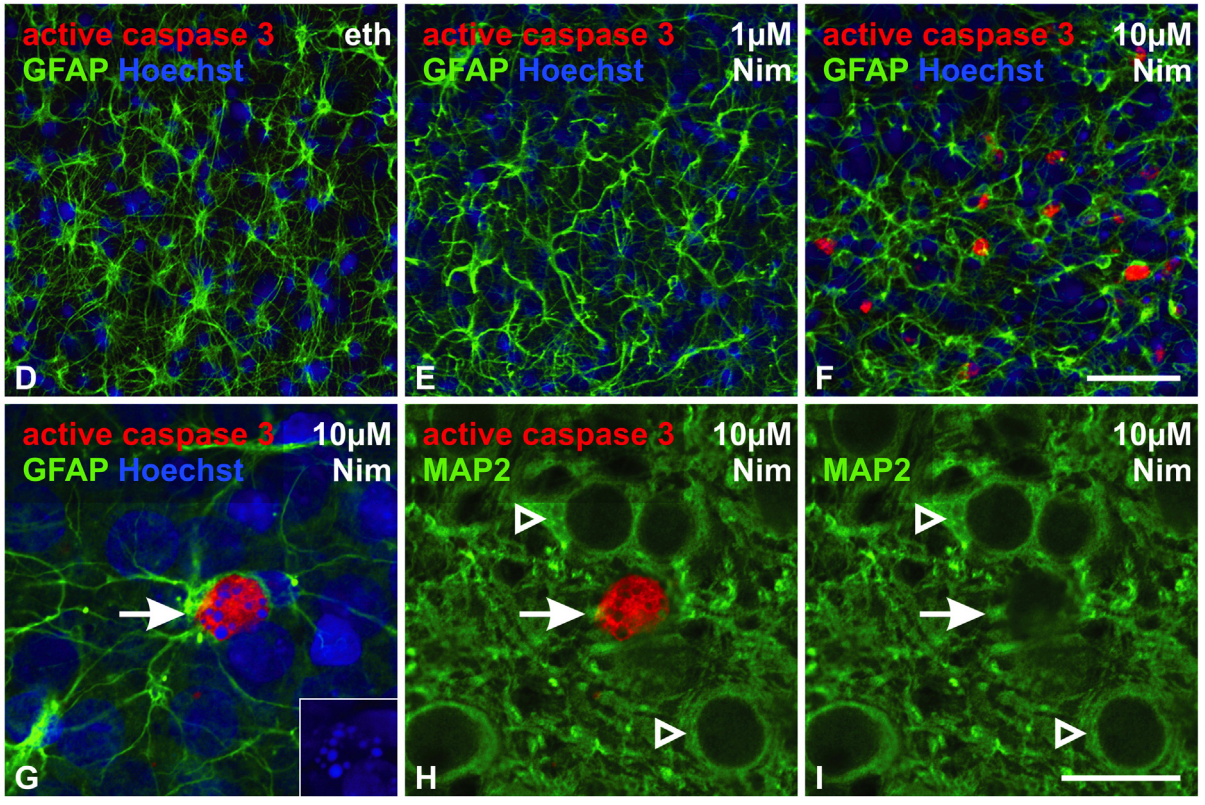

Fig. 3. Toxicity testing. (A) LDH release into 25% HS incubation medium. Data have been normalized to the control value at DIV1 of the respective preparation. Being maximal at DIV1, LDH activity decreased during the culture period without significant differences between the differently treated groups. (B) Propidium iodide uptake quantification in the co-cultures, shown as percentage of maximal damage after treatment with 10 mM glutamate. No significant changes were found after nimodipine (in the figure: Nim) application in comparison to the vehicle control ethanol (in the figure: eth). Data are shown as means, error bars indicate standard error, n(analyzed pictures) = 18, except glutamate: $n = 9$, $^{**}p < 0.01$, ANOVA followed by all pairwise multiple comparison procedures (Holm–Sidak test). (C) Quantification of active caspase 3 positive cells

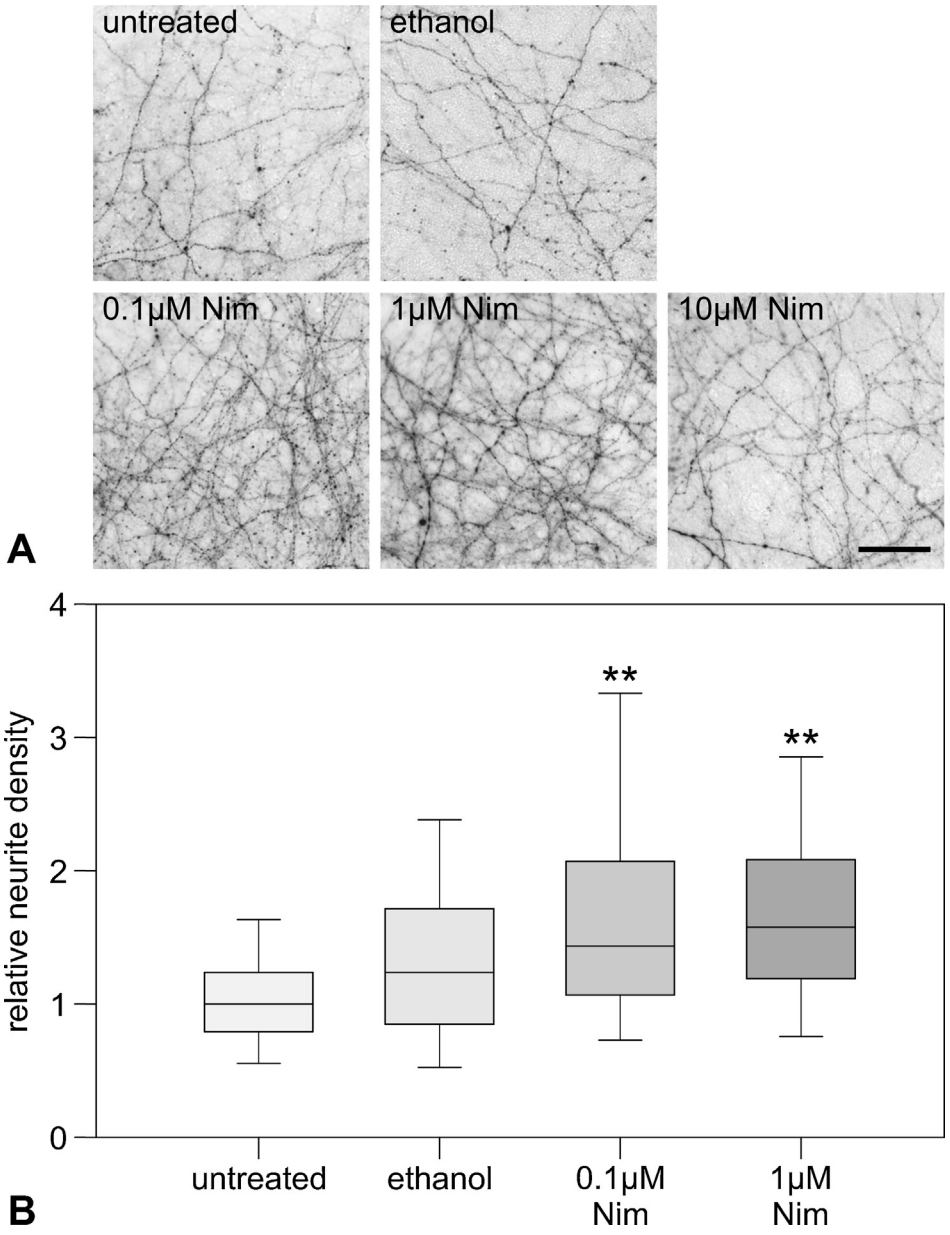

Fig. 4. Neurite outgrowth quantification. (A) Representative microscopic images of biocytin positive neurites in the border region, as they were used for neurite density quantification. For comparison and reference, an image of neurites treated with 10 μM nimodipine is included, (scale bar: 50 μm). (B) Neurite growth is significantly increased after treatment with 0.1 μM and 1 μM nimodipine (in the figure: Nim) in comparison to the vehicle control (0.1% ethanol). Neurite density data have been normalized to the median value of the untreated control group of each individual preparation. Data are shown as box plots, n(analyzed pictures) > 225, $^{**}p < 0.01$, ANOVA on ranks followed by all pairwise multiple comparison procedures (Dunn's test).

increased density of neurites in the border region of the co-cultures after application of nimodipine at certain concentrations (0.1 μM, 1 μM). The application of 10 μM nimodipine did not enhance neurite density. In contrast, we observed a moderate caspase 3 activation following application of 10 μM nimodipine. Moreover, we quantified the expression of several genes (CBPs, IEGs, GFAP and myelin constituents) in the co-cultures after incubation under the conditions, where enhanced neurite growth has been found. The expression of the investigated genes did not change significantly after treatment, indicating that other mechanisms are involved in the observed nimodipine mediated neurite growth.

(in the graph: active caspase 3^+ cells) in the cortical parts of the co-cultures detected by immunofluorescence staining. There are significantly more active caspase 3 positive cells found after application of 10 μM nimodipine, but not as pronounced as after application of 5 μM staurosporine (in the figure: sts), which served as a positive control for the induction of apoptosis. Data are shown as box plots, n(analyzed pictures) = 18, $^{*}p < 0.05$, $^{**}p < 0.01$, ANOVA on ranks followed by Dunn's multiple comparison against ethanol. (D–F) Confocal fluorescence microscopic images of the cortical part of the co-cultures after application of (E) 1 μM and (F) 10 μM nimodipine in comparison to (D) vehicle control ethanol. The number of active caspase 3 positive cells after treatment with 10 μM nimodipine is markedly increased. (G–I) Higher magnification of an active caspase 3 positive cell after treatment with 10 μM nimodipine; the active caspase 3 positive cell body (red, arrow) is surrounded by GFAP positive structures (green, G). Hoechst staining exhibits the fragmentation of the nucleus, typical for apoptotic cells, highlighted in the insert in (G). No clear co-localization with MAP2 (green, H and I) has been found, probably due to reduced immunoreactivity in apoptotic neurons (I). Active caspase 3 negative neurons with well-defined cell bodies are indicated by empty arrowheads. (Scale bars: D–F = 50 μm; G–I = 20 μm)

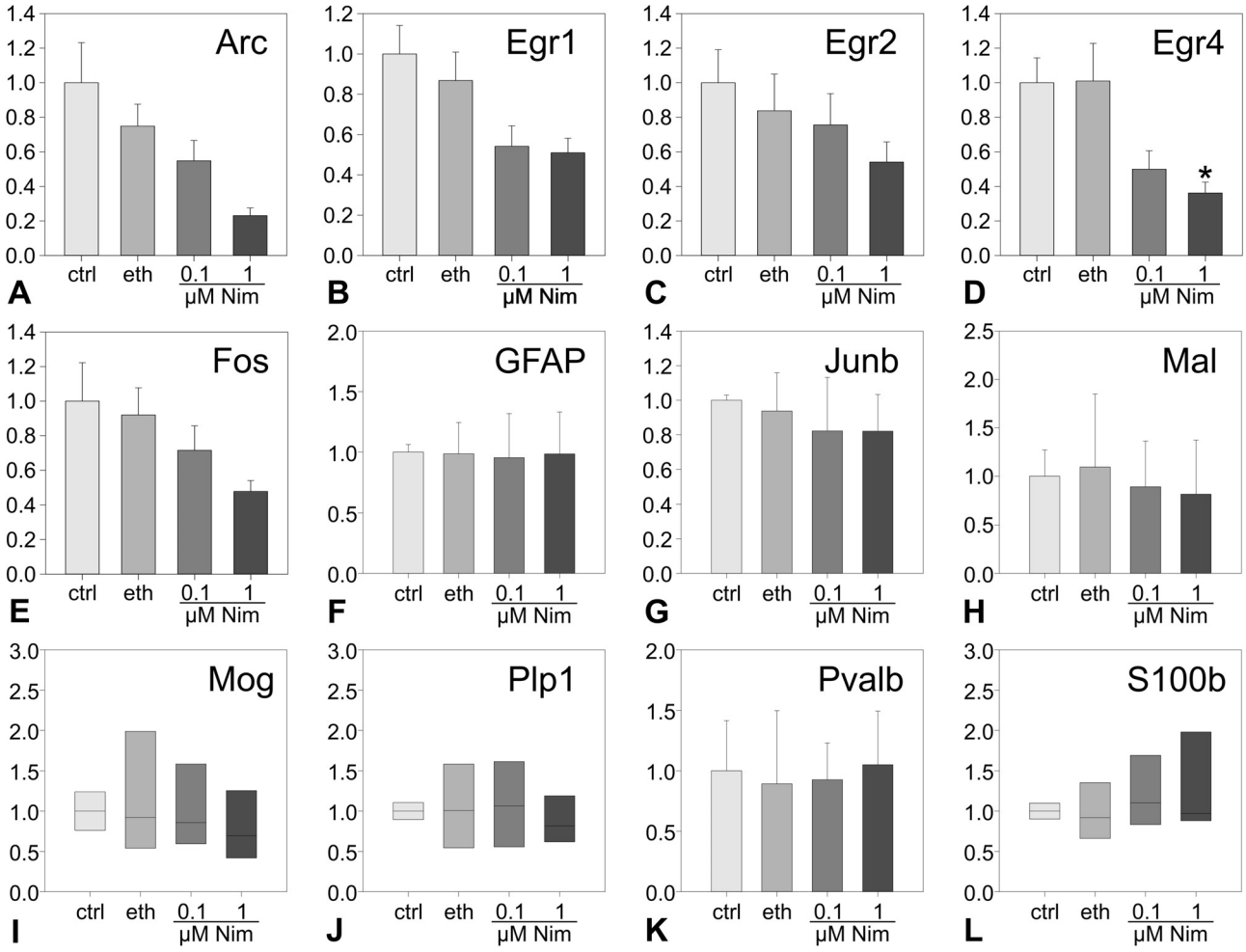

Fig. 5. Gene expression analysis in the PFC after treatment under "neurite growth promoting conditions". (A–E, G) Expression levels of immediate early genes decrease after application of 0.1 μM and 1 μM nimodipine. (F, H–L) Expression levels of GFAP, myelin constituents (Mal, Mog, Plp1) and Ca^{2+} binding proteins (Pvalb, S100b) are not significantly altered by nimodipine treatment under the applied conditions. Results are expressed as ΔCP, normalized to the untreated control (*y*-axis), while the *x*-axis represents the different treatments according to Fig. 1. *n*(independent samples) = 6, $^{*}p < 0.05$. (A–H, K) Data are shown as means, error bars indicate standard error, ANOVA followed by multiple comparisons *vs.* vehicle control ethanol (in the figure: eth), (Holm–Sidak test). (I, J, L) Data are shown as box plots, ANOVA on ranks; differences of expression levels were not significant.

4.1. Calcium and neurite growth

Axon outgrowth occurs within optimal levels of intracellular Ca^{2+}. If levels rise above or fall below a narrow optimal level growth is decelerated or inhibited (Kater et al., 1988). This suggests that nimodipine at concentrations of 0.1 μM and 1 μM – the concentrations that enhanced neurite density in our study – influences intracellular Ca^{2+} concentrations in a way that is optimal for neurite outgrowth in the used model. Even though it is not proven by our experiments, based on the published literature it seems very likely that Ca^{2+} is the causative agent in our model: LVCC play an active and specific role in mediating the effects of Ca^{2+} on growth cone motility and morphology, and different studies reported that Ca^{2+} influx through these channels affect axonal growth (Nishiyama et al., 2003; Schmitz et al., 2009; Tang et al., 2003). In addition, process extension is not only regulated by prolonged shifts in Ca^{2+} influx or intracellular baseline changes, but also by temporal intracellular Ca^{2+} fluctuations (Gomez and Zheng, 2006). Transient elevations of intracellular Ca^{2+} levels, either spontaneous or electrically stimulated, are known to affect neurite extension. It was shown that the incidence, frequencies, and amplitudes of Ca^{2+} transients are inversely related to the rate of axon outgrowth (Gomez et al., 1995; Gomez and Spitzer, 1999; Gu and Spitzer, 1995). This is consistent with our observations and the results of other studies, which have shown that partial blocking or silencing of Ca^{2+} influx by LVCC blockade accelerated axonal sprouting and outgrowth (Angelov et al., 1996; Lindsay et al., 2010; Mattsson et al., 2001).

As already mentioned above, the concentration of the applied LVCC blockers seems to be crucial. Daschil and Humpel (2014) have shown a dose-dependent effect of LVCC blockers on the survival of SN *pars compacta* neurons in dopaminergic brain slices. Among the tested concentrations (0.1 μM, 1 μM and 10 μM), only 1 μM and 10 μM nifedipine and 1 μM nimodipine markedly enhanced the survival of SN neurons. In addition, after blockade of LVCC with nifedipine at increasing concentrations (5–30 μM), Tang et al. (2003) observed increased axon lengths of cortical neurons in cell culture experiments. They also applied nimodipine (10 μM) and found neurite growth enhancement. In contrast, we did not find growth promotion, but rather toxic effects with nimodipine used at this concentration. This discrepancy likely relates to differences between the two model systems and application schemes (single *versus* repeated long-term application). The latter is especially likely to be a relevant difference as Koh and Cotman (1992) reported that prolonged LVCC blockade has detrimental effects on neurons.

4.2. Neuroprotection and neurotoxicity

In this study, we focused on the regenerative and growth promoting potential of nimodipine in the dopaminergic system. However, parameters of neuroprotection have also been analyzed. The absence of a reduction of LDH release in the nimodipine (0.1 μM, 1 μM, 10 μM) treated samples after the preparation of the brain slices (representing a mechanical insult with deterioration of neuronal connections) does not suggest a neuroprotective effect of nimodipine in the used experimental model. In contrast, quantification of active caspase 3 after nimodipine (10 μM) application revealed the induction of apoptosis.

Recently, it was reported that 10 μM nimodipine is toxic to cultured hippocampal neurons (Sendrowski et al., 2013). Additionally, high concentrations and prolonged administration of LVCC blockers like nimodipine have been reported to be toxic in primary cell cultures (Koh and Cotman, 1992) and *in vivo* (Turner et al., 2007). There is an increased vulnerability to Ca^{2+} deprivation especially within a tight time window during postnatal neuronal development (around P7) (Turner et al., 2007).

Moreover, Puopolo et al. (2007) have found that nimodipine (3 μM) completely blocks spontaneous firing in acutely dissociated SN pars compacta neurons, and Mercuri et al. (1994) did show in mesencephalic brain slice cultures that spontaneous electrical activity of dopaminergic neurons is blocked by the application of 10 μM nimodipine. It is widely accepted that electrical activity is a prerequisite for neuronal survival and its blockade leads to programmed cell death (as reviewed by Mennerick and Zorumski, 2000). Therefore, we suggest that the observed caspase 3 activation and the absence of enhanced neurite growth in the co-cultures after application of 10 μM nimodipine could be a result of the reduced electrical activity (due to the LVCC blockade).

With multiple fluorescence labeling after application of 10 μM nimodipine, we found active caspase 3 immunoreactivity located in areas where MAP2 staining is less defined compared to the surroundings where MAP2 staining is distinctly demarcated. Therefore, our interpretation of the multiple immunofluorescence labeling is that presumably neurons undergoing apoptosis following LVCC blockade by 10 μM nimodipine. This is in line with other reports, indicating that disappearance of MAP2 can be used as a marker for neurotoxic events (Koczyk, 1994). Moreover, earlier studies demonstrated that only neurons – not glial cells – are vulnerable to higher concentrations of nimodipine (Koh and Cotman, 1992). We suggest that the GFAP positive structures surrounding active caspase 3 positive cell bodies most likely belong to reactive astrocytes, which envelop apoptotic neurons and thereby isolate the dying cells from the environment.

4.3. Nimodipine's mode of action and target cells

To elucidate the mechanism leading to the reported beneficial effects of nimodipine, gene expression has been analyzed using expression microarrays. We found a group of genes belonging to IEGs to be upregulated in the nimodipine treated PFC samples. Given that (i) the PFC is the target region of the dopaminergic neurite processes and therefore the region where new connections are established; (ii) the PFC is supposed to produce guiding signals that trigger neurite ingrowth (Gomez-Urquijo et al., 1999; Plenz and Kitai, 1996) and (iii) changes in gene expression in the VTA/SN following nimodipine application were not found in the applied model, we focused on the PFC samples for further gene expression analyses.

Applying qPCR after culture under the conditions promoting enhanced neurite growth, we pursued the leads from other published investigations and interpreted our own preliminary microarray analysis as discussed below:

Transient upregulation of Pvalb and S100b until P10 was observed in the neocortex and the hippocampus after maternal perinatal nimodipine administration in rats (Buwalda et al., 1994). This upregulation of CBPs was supposed to be one of the mechanisms that lead to the observed neuroprotective effect of nimodipine after perinatally occurring ischemic insults. We did not find such an increase in transcripts encoding for the chosen CBPs (Pvalb, S100b) in response to nimodipine treatment in the cortical part of the co-cultures at the end of the culture period.

LVCC are also present on glia (D'Ascenzo et al., 2004; Latour et al., 2003; Westenbroek et al., 1998). It was shown that long-term treatment with nimodipine (*in vivo*, >42 days) led to enhanced and prolonged astroglial ensheathment of axotomized, target deprived neurons in an *in vivo* model of facial and hypoglossal nerve resection, (Guntinas-Lichius et al., 1997). It was further shown that nimodipine reduced cell loss and increased GFAP immunoreactivity in a model of traumatic brain injury (Thomas et al., 2008). However, quantification of GFAP encoding mRNA transcripts did not reveal changes of gene expression levels in our model at DIV11.

In addition, application of nimodipine increased not only the number and size of myelinated axons of the facial nerve but also increased the degree of myelination, both in lesioned and non-lesioned facial nerves (Mattsson et al., 2001). In order to explore whether nimodipine application affects myelination and thereby stabilizes axonal growth in our model, we quantified the transcripts of the myelin components Mal, Mog and Plp1. No significant gene expression changes have been found, suggesting that this aspect is not relevant for the enhanced neurite growth observed in dopaminergic brain slice co-cultures.

In the microarray and qPCR analysis, we found IEGs to be upregulated after 10 μM nimodipine application. We wanted to confirm this upregulation under the conditions that enhanced neurite outgrowth. IEGs are closely related to neuronal growth and plasticity and therefore are interesting candidates for the regulation of neurite growth (reviewed in Pérez-Cadahía et al., 2011; Shepherd and Bear, 2011). However, the findings from the microarray analysis were not reproduced after application of 0.1 μM or 1 μM nimodipine. In contrast, we found a decrease in expression levels after nimodipine (0.1 μM, 1 μM) treatment. The down-regulating effect of a dihydropyridine LVCC blocker on the expression of IEGs (*e.g.* c-Fos, JunB, Egr1 and others) is in line with the results of Murphy et al. in cultured cortical neurons (Murphy et al., 1991) and with the findings reviewed by Sheng and Greenberg, which demonstrated an upregulation of these genes not only after stimulation with growth factors (NGF and Epidermal Growth Factor, EGF) but also after Ca^{2+} influx and depolarization (Sheng and Greenberg, 1990). This study further corroborates the notion that blockade of Ca^{2+} influx inhibits IEG expression rather than induces it.

In summary, the results of the gene expression analysis indicate that the regulation of the expression of the investigated genes cannot clearly explain the observed nimodipine mediated neurite growth in the applied model of the dopaminergic projection system. Therefore, referring to the investigated genes, nimodipine-induced neurite outgrowth does not seem to depend on mRNA synthesis. In contrast, mechanisms including non-coding RNA or nimodipine-induced protein modifications should be considered and examined in further investigations.

4.4. Conclusion and translational outlook

Nimodipine – at certain concentrations (0.1 μM, 1 μM) – seems to influence the intracellular Ca^{2+} concentration in a way

Table A.1
Sequences of primers for quantitative polymerase chain reaction (qPCR).

Target	Accession ID	Forward primer	Reverse primer
Genes of interest			
Arc	NM_019361.1	GCCAGTCTTGGGCAGCATAG	CACTGGTATGAATCACTGCTGG
Bax	NM_017059.2	ACCCGGCGAGAGGCAG	CTCGATCCTGGATGAAACCCT
Bcl-2	NM_016993.1	GACTGAGTACCTGAACCGGC	AGTTCCACAAAGGCATCCCAG
Egr1	NM_012551.2	ACCTGACCACAGAGTCCTTTTC	GCAACCGGGTAGTTTGGCT
Egr2	NM_053633.1	CTACCCGGTGGAAGACCTCG	GATCATGCCATCTCCAGCCAC
Egr4	NM_019137.1	TATCCTGGAGGCGACTTCTTG	TCCAGGAAGCAGGAGTCTGTT
Fos	NM_022197.2	TACTACCATTCCCCAGCCGA	CTGCGCAAAAGTCCTGTGTG
Junb	NM_021836.2	AGGCAGCTACTTTTCGGGTC	TTGCTGTTGGGGACGATCAA
Gfap	NM_017009.2	AGCTTACTACCAACAGTGCCC	TCATCTTGGAGCTTCTGCCTC
Mal	NM_012798.1	CTGCAGTGGTGTTCGCCTAT	GCTCCCAATCTGCTGTCCTA
Mog	NM_022668.2	TGTGTGGAGCCTTTCTCTGC	TGAACTGTCCTGCGTAGCTG
Plp1	NM_030990.2	CTGCAAAACAGCCGAGTTCC	AGGGAAACTAGTGTGGCTGC
Pvalb	NM_022499	AAGAGTGCGGATGATGTGAAGA	CAGAATGGACCCCAGCTCATC
S100b(eta)	NM_013191.1	AGAGGGTGACAAGCACAAGC	TTCCTGCTCTTTGATTTCCTCCA
Housekeeping genes			
MrpL32	NM_001106116.1	TTCCGGACCGCTACATAGGTG	CTAGTGCTGGTGCCCACTGAG
Ubc	NM_017314.1	ACACCAAGAAGGTCAAACAGGA	CACCTCCCCATCAAACCCAA

that is advantageous for neurite outgrowth. Thereby nimodipine enhances neurite density in organotypic co-cultures of the dopaminergic projection system, as demonstrated for the first time in this study.

In addition, we did show that a set of genes whose expression levels were quantified are not changed by nimodipine application, suggesting that other mechanisms are involved in the observed nimodipine mediated effects.

The here presented data support previous clinical observations of the beneficial effect of nimodipine *e.g.* on the preservation of cranial nerve functions following vestibular schwannoma surgery (Scheller et al., 2007). Regarding the use of nimodipine against diseases affecting especially the dopaminergic system, primarily further *in vivo* data and eventually clinical studies will have to be conducted. In general, nimodipine is a usually well-tolerated drug (Castanares-Zapatero and Hantson, 2011). Therefore no barriers in the use of nimodipine for neurite outgrowth in clinical situations are expected. The elucidation of the detailed mode of action of nimodipine as a neuroprotective and neuroregeneration promoting substance – especially within the dopaminergic projection system – will help to foster its application and the identification of new targets and therapy options also within the dopaminergic projection system.

Acknowledgements

The authors thank Katrin Becker and Anne-Kathrin Krause (Rudolf Boehm Institute of Pharmacology and Toxicology) for technical assistance. We thank Dr. Martin Reinsch at the Analytisches Zentrum Biopharm GmbH (Berlin, Germany) for quantifying the nimodipine concentrations in the co-culture tissues. The authors are grateful to Dr. Knut Krohn and the members of the microarray core facility of the Interdisziplinäres Zentrum für klinische Forschung (IZKF) Leipzig (Faculty of Medicine, University of Leipzig) for performing the microarray measurements. We also thank Christin Zöller for her secretarial contribution and Jennifer Ding for providing language help. The work presented in this paper was made possible by funding from the German Federal Ministry of Education and Research (BMBF 1315883). Furthermore, the study was supported by Bayer Vital GmbH (Leverkusen, Germany). The funding sources have not been involved in the study design, in the collection, analysis and interpretation of data; in the writing of the report; or in the decision to submit the article for publication.

Appendix A.

Table A.1

References

Angelov, D.N., Neiss, W.F., Streppel, M., Andermahr, J., Mader, K., Stennert, E., 1996. Nimodipine accelerates axonal sprouting after surgical repair of rat facial nerve. J. Neurosci. 16, 1041–1048.

Bartrup, J.T., Stone, T.W., 1990. Dihydropyridines alter adenosine sensitivity in the rat hippocampal slice. Br. J. Pharmacol. 101, 97–102.

Blanc, E.M., Bruce-Keller, A.J., Mattson, M.P., 1998. Astrocytic gap junctional communication decreases neuronal vulnerability to oxidative stress-induced disruption of Ca^{2+} homeostasis and cell death. J. Neurochem. 70, 958–970.

Buwalda, B., Naber, R., Nyakas, C., Luiten, P.G., 1994. Nimodipine accelerates the postnatal development of parvalbumin and S-100 beta immunoreactivity in the rat brain. Brain Res. Dev. Brain Res. 78, 210–216.

Castanares-Zapatero, D., Hantson, P., 2011. Pharmacological treatment of delayed cerebral ischemia and vasospasm in subarachnoid hemorrhage. Ann. Intens. Care 1, 12.

D'Ascenzo, M., Vairano, M., Andreassi, C., Navarra, P., Azzena, G.B., Grassi, C., 2004. Electrophysiological and molecular evidence of L-(Cav1), N-(Cav2.2), and R-(Cav2.3) type Ca^{2+} channels in rat cortical astrocytes. Glia 45, 354–363.

Daschil, N., Humpel, C., 2014. Nifedipine and nimodipine protect dopaminergic substantia nigra neurons against axotomy-induced cell death in rat vibrosections via modulating inflammatory responses. Brain Res. 1581, 1–11.

Dolmetsch, R.E., Pajvani, U., Fife, K., Spotts, J.M., Greenberg, M.E., 2001. Signaling to the nucleus by an L-type calcium channel-calmodulin complex through the MAP kinase pathway. Science 294, 333–339.

Fields, R.D., Guthrie, P.B., Russell, J.T., Kater, S.B., Malhotra, B.S., Nelson, P.G., 1993. Accommodation of mouse DRG growth cones to electrically induced collapse: kinetic analysis of calcium transients and set-point theory. J. Neurobiol. 24, 1080–1098.

Franke, H., Schelhorn, N., Illes, P., 2003. Dopaminergic neurons develop axonal projections to their target areas in organotypic co-cultures of the ventral mesencephalon and the striatum/prefrontal cortex. Neurochem. Int. 42, 431–439.

Gispen, W.H., Schuurman, T., Traber, J., 1988. Nimodipine and neural plasticity in the peripheral nervous system of adult and aged rats. In: Morad, M., Nayler, W., Kazda, S., Schramm, M. (Eds.), The Calcium Channel: Structure, Function and Implications. Springer, New York, pp. 491–502.

Gomez, T.M., Snow, D.M., Letourneau, P.C., 1995. Characterization of spontaneous calcium transients in nerve growth cones and their effect on growth cone migration. Neuron 14, 1233–1246.

Gomez, T.M., Spitzer, N.C., 1999. In vivo regulation of axon extension and pathfinding by growth-cone calcium transients. Nature 397, 350–355.

Gomez, T.M., Zheng, J.Q., 2006. The molecular basis for calcium-dependent axon pathfinding. Nat. Rev. Neurosci. 7, 115–125.

Gomez-Urquijo, S.M., Hökfelt, T., Ubink, R., Lubec, G., Herrera-Marschitz, M., 1999. Neurocircuitries of the basal ganglia studied in organotypic cultures: focus on tyrosine hydroxylase, nitric oxide synthase and neuropeptide immunocytochemistry. Neuroscience 94, 1133–1151.

Gu, X., Spitzer, N.C., 1995. Distinct aspects of neuronal differentiation encoded by frequency of spontaneous Ca^{2+} transients. Nature 375, 784–787.

Guntinas-Lichius, O., Martinez-Portillo, F., Lebek, J., Angelov, D.N., Stennert, E., Neiss, W.F., 1997. Nimodipine maintains in vivo the increase in GFAP and enhances the

astroglial ensheathment of surviving motoneurons in the rat following permanent target deprivation. J. Neurocytol. 26, 241–248.
Harkany, T., Dijkstra, I.M., Oosterink, B.J., Horvath, K.M., Abrahám, I., Keijser, J., van der Zee, E.A., Luiten, P.G., 2000. Increased amyloid precursor protein expression and serotonergic sprouting following excitotoxic lesion of the rat magnocellular nucleus basalis: neuroprotection by Ca(2+) antagonist nimodipine. Neuroscience 101, 101–114.
Heine, C., Wegner, A., Grosche, J., Allgaier, C., Illes, P., Franke, H., 2007. P2 receptor expression in the dopaminergic system of the rat brain during development. Neuroscience 149, 165–181.
Heine, C., Sygnecka, K., Scherf, N., Berndt, A., Egerland, U., Hage, T., Franke, H., 2013. Phosphodiesterase 2 inhibitors promote axonal outgrowth in organotypic slice co-cultures. Neurosignals 21, 197–212.
Heine, C., Franke, H., 2014. An ex vivo organotypic culture system to study axon regeneration in the dopaminergic system. In: Axon Growth and Regeneration: Methods and Protocols. Humana Press, Springer, Clifton, N.J.
Kater, S.B., Mattson, M.P., Cohan, C., Connor, J., 1988. Calcium regulation of the neuronal growth cone. Trends Neurosci. 11, 315–321.
Kater, S.B., Mills, L.R., 1991. Regulation of growth cone behavior by calcium. J. Neurosci. 11, 891–899.
Kobayashi, T., Mori, Y., 1998. Ca^{2+} channel antagonists and neuroprotection from cerebral ischemia. Eur. J. Pharmacol. 363, 1–15.
Koczyk, D., 1994. Differential response of microtubule-associated protein 2 (MAP-2) in rat hippocampus after exposure to trimethyltin (TMT): an immunocytochemical study. Acta Neurobiol. Exp. (Wars) 54, 55–58.
Koh, J.Y., Choi, D.W., 1987. Quantitative determination of glutamate mediated cortical neuronal injury in cell culture by lactate dehydrogenase efflux assay. J. Neurosci. Methods 20, 83–90.
Koh, J.Y., Cotman, C.W., 1992. Programmed cell death: its possible contribution to neurotoxicity mediated by calcium channel antagonists. Brain Res. 587, 233–240.
Krieglstein, J., Lippert, K., Pöch, G., 1996. Apparent independent action of nimodipine and glutamate antagonists to protect cultured neurons against glutamate-induced damage. Neuropharmacology 35, 1737–1742.
Latour, I., Hamid, J., Beedle, A.M., Zamponi, G.W., Macvicar, B.A., 2003. Expression of voltage-gated Ca^{2+} channel subtypes in cultured astrocytes. Glia 41, 347–353.
Lecht, S., Rotfeld, E., Arien-Zakay, H., Tabakman, R., Matzner, H., Yaka, R., Lelkes, P.I., Lazarovici, P., 2012. Neuroprotective effects of nimodipine and nifedipine in the NGF-differentiated PC12 cells exposed to oxygen-glucose deprivation or trophic withdrawal. Int. J. Dev. Neurosci. 30, 465–469.
Li, Y., Hu, X., Liu, Y., Bao, Y., An, L., 2009. Nimodipine protects dopaminergic neurons against inflammation-mediated degeneration through inhibition of microglial activation. Neuropharmacology 56, 580–589.
Lindsay, R.W., Heaton, J.T., Edwards, C., Smitson, C., Hadlock, T.A., 2010. Nimodipine and acceleration of functional recovery of the facial nerve after crush injury. Arch. Facial Plast. Surg. 12, 49–52.
Liu, G.J., Luo, J., Zhang, L.P., Wang, Z.J., Xu, L.L., He, G.H., Zeng, Y.J., Wang, Y.F., 2011. Meta-analysis of the effectiveness and safety of prophylactic use of nimodipine in patients with an aneurysmal subarachnoid haemorrhage. CNS Neurol. Disord. Drug Targets 10, 834–844.
Luiten, P.G., Buwalda, B., Traber, J., Nyakas, C., 1994. Induction of enhanced postnatal expression of immunoreactive calbindin-D28k in rat forebrain by the calcium antagonist nimodipine. Brain Res. Dev. Brain Res. 79, 10–18.
Martínez-Sánchez, M., Striggow, F., Schröder, U.H., Kahlert, S., Reymann, K.G., Reiser, G., 2004. Na^{+} and Ca^{2+} homeostasis pathways, cell death and protection after oxygen–glucose-deprivation in organotypic hippocampal slice cultures. Neuroscience 128, 729–740.
Mattsson, P., Janson, A.M., Aldskogius, H., Svensson, M., 2001. Nimodipine promotes regeneration and functional recovery after intracranial facial nerve crush. J. Comp. Neurol. 437, 106–117.
Mennerick, S., Zorumski, C.F., 2000. Neural activity and survival in the developing nervous system. Mol. Neurobiol. 22, 41–54.
Mercuri, N.B., Bonci, A., Calabresi, P., Stratta, F., Stefani, A., Bernardi, G., 1994. Effects of dihydropyridine calcium antagonists on rat midbrain dopaminergic neurones. Br. J. Pharmacol. 113, 831–838.
Murphy, T.H., Worley, P.F., Baraban, J.M., 1991. L-type voltage-sensitive calcium channels mediate synaptic activation of immediate early genes. Neuron 7, 625–635.
Nedergaard, S., Flatman, J.A., Engberg, I., 1993. Nifedipine- and omega-conotoxin-sensitive Ca^{2+} conductances in guinea-pig *Substantia nigra* pars compacta neurones. J. Physiol. (Lond.) 466, 727–747.
Nishiyama, M., Hoshino, A., Tsai, L., Henley, J.R., Goshima, Y., Tessier-Lavigne, M., Poo, M., Hong, K., 2003. Cyclic AMP/GMP-dependent modulation of Ca^{2+} channels sets the polarity of nerve growth-cone turning. Nature 423, 990–995.
Opgen-Rhein, R., Strimmer, K., 2007. Accurate ranking of differentially expressed genes by a distribution-free shrinkage approach. Stat. Appl. Genet. Mol. Biol. 6, Article9.
Pérez-Cadahía, B., Drobic, B., Davie, J.R., 2011. Activation and function of immediate-early genes in the nervous system. Biochem. Cell Biol. 89, 61–73.
Pisani, A., Calabresi, P., Tozzi, A., D'Angelo, V., Bernardi, G., 1998. L-type Ca^{2+} channel blockers attenuate electrical changes and Ca^{2+} rise induced by oxygen/glucose deprivation in cortical neurons. Stroke 29, 196–202.
Plenz, D., Kitai, S.T., 1996. Organotypic cortex-striatum-mesencephalon cultures: the nigrostriatal pathway. Neurosci. Lett. 209, 177–180.
Pozzo-Miller, L.D., Inoue, T., Murphy, D.D., 1999. Estradiol increases spine density and NMDA-dependent Ca^{2+} transients in spines of CA1 pyramidal neurons from hippocampal slices. J. Neurophysiol. 81, 1404–1411.
Puopolo, M., Raviola, E., Bean, B.P., 2007. Roles of subthreshold calcium current and sodium current in spontaneous firing of mouse midbrain dopamine neurons. J. Neurosci. 27, 645–656.
Quirion, R., Lal, S., Nair, N.P., Stratford, J.G., Ford, R.M., Olivier, A., 1985. Comparative autoradiographic distribution of calcium channel antagonist binding sites for 1,4-dihydropyridine and phenylalkylamine in rat, guinea pig and human brain. Prog. Neuropsychopharmacol. Biol. Psychiatry 9, 643–649.
Rami, A., Krieglstein, J., 1994. Neuronal protective effects of calcium antagonists in cerebral ischemia. Life Sci. 55, 2105–2113.
Scheller, C., Richter, H., Engelhardt, M., Köenig, R., Antoniadis, G., 2007. The influence of prophylactic vasoactive treatment on cochlear and facial nerve functions after vestibular schwannoma surgery: a prospective and open-label randomized pilot study. Neurosurgery 61, 92–98.
Scheller, K., Scheller, C., 2012. Nimodipine promotes regeneration of peripheral facial nerve function after traumatic injury following maxillofacial surgery: an off label pilot-study. J. Craniomaxillofac. Surg. 40, 427–434.
Scheller, C., Vogel, A., Simmermacher, S., Rachinger, J.C., Prell, J., Strauss, C., Reinsch, M., Kunter, U., Wienke, A., Neumann, Scheller, K., 2012. Prophylactic intravenous nimodipine treatment in skull base surgery: pharmacokinetic aspects. J. Neurol. Surg. A: Cent. Eur. Neurosurg. 73, 153–159.
Schmitz, Y., Luccarelli, J., Kim, M., Wang, M., Sulzer, D., 2009. Glutamate controls growth rate and branching of dopaminergic axons. J. Neurosci. 29, 11973–11981.
Sendrowski, K., Rusak, M., Sobaniec, P., Iłendo, E., Dąbrowska, M., Boćkowski, L., Koput, A., Sobaniec, W., 2013. Study of the protective effect of calcium channel blockers against neuronal damage induced by glutamate in cultured hippocampal neurons. Pharmacol. Rep. 65, 730–736.
Sheng, M., Greenberg, M.E., 1990. The regulation and function of c-fos and other immediate early genes in the nervous system. Neuron 4, 477–485.
Shepherd, J.D., Bear, M.F., 2011. New views of Arc, a master regulator of synaptic plasticity. Nat. Neurosci. 14, 279–284.
Takada, M., Kang, Y., Imanishi, M., 2001. Immunohistochemical localization of voltage-gated calcium channels in substantia nigra dopamine neurons. Eur. J. Neurosci. 13, 757–762.
Tang, F., Dent, E.W., Kalil, K., 2003. Spontaneous calcium transients in developing cortical neurons regulate axon outgrowth. J. Neurosci. 23, 927–936.
Thomas, S., Herrmann, B., Samii, M., Brinker, T., 2008. Experimental subarachnoid hemorrhage in the rat: influences of nimodipine. Acta Neurochir. Suppl. 102, 377–379.
Törönen, P., Ojala, P.J., Marttinen, P., Holm, L., 2009. Robust extraction of functional signals from gene set analysis using a generalized threshold free scoring function. BMC Bioinform. 10, 307.
Turner, C.P., Miller, R., Smith, C., Brown, L., Blackstone, K., Dunham, S.R., Strehlow, R., Manfredi, M., Slocum, P., Iverson, K., West, M., Ringler, S.L., 2007. Widespread neonatal brain damage following calcium channel blockade. Dev. Neurosci. 29, 213–231.
Weiss, J.H., Pike, C.J., Cotman, C.W., 1994. Ca^{2+} channel blockers attenuate beta-amyloid peptide toxicity to cortical neurons in culture. J. Neurochem. 62, 372–375.
Westenbroek, R.E., Bausch, S.B., Lin, R.C., Franck, J.E., Noebels, J.L., Catterall, W.A., 1998. Upregulation of L-type Ca^{2+} channels in reactive astrocytes after brain injury, hypomyelination, and ischemia. J. Neurosci. 18, 2321–2334.
Wirth, H., von Bergen, M., Binder, H., Mining, S.O.M., 2012. expression portraits: feature selection and integrating concepts of molecular function. Biodata Mining 5, 18.